Stimulated oxygen impurity gettering under ultra-shallow junction formation in silicon

2014 Semicond. Sci. Technol. 29 055008

IOP Publishing Semiconductor Science and Technology
Semicond. Sci. Technol. **29** (2014) 055008 (7pp) doi:10.1088/0268-1242/29/5/055008

Stimulated oxygen impurity gettering under ultra-shallow junction formation in silicon

O Oberemok[1], V Kladko[1], V Litovchenko[1], B Romanyuk[1], V Popov[1], V Melnik[1], A Sarikov[1], O Gudymenko[1] and J Vanhellemont[2]

[1] V. Lashkarev Institute of Semiconductor Physics NAS of Ukraine, 41 Prospect Nauki, 03028 Kyiv, Ukraine
[2] Department of Solid State Sciences, Ghent University, Krijgslaan 281 S1, B-9000 Ghent, Belgium

E-mail: ober@isp.kiev.ua, kladko@isp.kiev.ua, lvg@isp.kiev.ua, romb@isp.kiev.ua, sarikov@isp.kiev.ua and jan.vanhellemont@ugent.be

Received 24 January 2014, revised 18 March 2014
Accepted for publication 21 March 2014
Published 16 April 2014

Abstract

Ultra-shallow junctions were formed by low-energy As ion implantation followed by furnace annealing. It was found that a significant amount of oxygen is redistributed from the silicon bulk to the As-implanted region. Using a marker layer created by implantation of ^{18}O isotope, it is confirmed that a large number of interstitial oxygen atoms are transferred from the bulk of Si wafer to the surface during dopant activation annealing, which leads to an increase of the surface oxide thickness. Estimation of the oxygen diffusivity in silicon during the 950 °C anneal, yields a value close to 1×10^{-10} cm^2 s^{-1} which is more than an order of magnitude larger than the literature value which is close to 7×10^{-12} cm^2 s^{-1}.

Keywords: ion implantation, impurities, p-n junctions, annealing, depth profile, oxygen, arsenic, gettering

(Some figures may appear in colour only in the online journal)

Introduction

The processes for formation of the source/drain regions in metal-oxide-semiconductor field effect transistors become increasingly important as device dimensions are scaled down. In order to suppress the short-channel effect, creation of the ultra-shallow junction (USJ) with high dopant activation is required [1]. In particular, low-energy implantation of As is widely used to create the n-type region. However, formation of USJ is complicated by the dopant deactivation and its accumulation near the SiO_2–Si interface [2], and transient-enhanced diffusion as a result of interaction with point defects [3]. Directions to overcome these problems are discussed in many papers [4–6]. Another important factor affecting the properties of the USJ in Czochralski Si is oxygen impurities. It is known that oxygen precipitation in silicon leads to formation of defects that act as gettering centers for impurities, responsible for the leakage current [7, 8]. Also, oxygen precipitation is strongly dependent on the presence of vacancies generated by ion implantation and existing mechanical stresses under various thermal treatments [9]. Oxygen is rapidly gettered into residual damage regions, forming stable SiO_x precipitates during annealing [10]. It was found [11] that compared with that in lightly doped wafers, oxygen precipitation was enhanced in B-doped wafers and was retarded in As-doped wafers during the annealing process. It was previously shown that the high-energy implanted As can influence stoichiometry of screen oxide [12]. A local increase of the oxygen concentration above 10^{20} cm^{-3} in the As shallow junction leads to degradation of electrical characteristics and reduction of the carrier mobility [13]. The reason for this behavior is formation of electrically inactive As–O [14] or O–As–V clusters [15]. All these factors lead to degradation of the devices. Unfortunately, information about oxygen behavior near the USJ is almost absent for the ion implantation of these dopants.

In this work, USJs were created in the course of low-energy As^+ implantation with the subsequent high-temperature annealing. The As and oxygen redistributions were studied using the SIMS method. The buried oxygen marker layer was used for a verification of the oxygen diffusion toward the As distribution region. The marker layer

was created by ion implantation of ^{18}O oxygen isotope. The physical model for oxygen redistribution accounting for nonequilibrium defects and mechanical stress influences has been proposed.

Experiment

All the experiments were performed on (1 0 0) p-type 10 Ω × cm Czochralski-grown silicon wafers containing about 10^{18} cm^{-3} interstitial oxygen atoms, according to the specifications. FTIR measurements of the light absorption coefficient αOi at the frequency 1107 cm^{-1} were performed on some of the samples to confirm this concentration. Using the expression Oi = 3.14 × 1017αOi, the measured interstitial oxygen concentration Oi agreed with the specified one within 10% accuracy. The samples were ion implanted through the 2.2 nm screen oxide with 4 × 10^{14} cm^{-2}, 5 keV As^+. Furnace annealing of the As-implanted samples was carried out in nitrogen ambient for 0.5 to 20 min within the temperature range 750 to 950 °C. The time to reach the 'annealing temperatures' was 25 s for 750 °C and 35 s for 950 °C. Square, 1 × 1 cm^2, samples were used for all experiments. Some of the samples were additionally ion implanted with ^{18}O (100 keV, 1.2 × 10^{14} cm^{-2}). Analysis of the dopant depth profiles was performed using secondary ion mass spectroscopy (SIMS) with a Cameca IMS 4F instrument. The precise component analysis of thin surface layers was made with time of flight-SIMS IV instrument by using low-energy (0.4 keV) Cs^+ ion sputtering. The depth scale was determined for each profile by measuring the crater depth with the Dektak 3030 profilometer. Peculiarities of defect creation and transformation were investigated using the x-ray diffuse scattering (XDS) technique with the high-resolution diffractometer PANalytical X'Pert Pro MRD. The XDS intensity distribution $I(q)$ was measured in the vicinity of the 0 0 4 node [16].

Results and discussion

SIMS depth profiles of As and $^{60}SiO_2$ in Si before and after annealing at the temperatures 750 to 950 °C for 5 min are shown in figure 1. It is seen that after annealing the implanted As is redistributed both toward the surface and into the bulk of the sample. After annealing at 750 °C, only a small shift of As distribution maximum toward the SiO_2/Si interface is observed. Increasing the annealing temperature leads to enhanced As diffusion and As pile-up at the SiO_2/Si interface. As accumulation at the SiO_2/Si interface is increasing with annealing temperature and duration. It was also found that As redistribution is accompanied by changes in the oxygen concentration in the vicinity of USJ location. In the following we call this region the active diffusion region (ADR) of impurities that is located between 3 (SiO_2/Si interface) and 100 nm below the wafer surface.

The oxygen concentration depth distribution between 40 to 60 nm below the surface is shown in the inset to figure 1 for anneals at 750, 850 and 950 °C for 5 min. One can see that the oxygen concentration in this region substantially increases, with decreasing anneal temperature. The oxygen detection

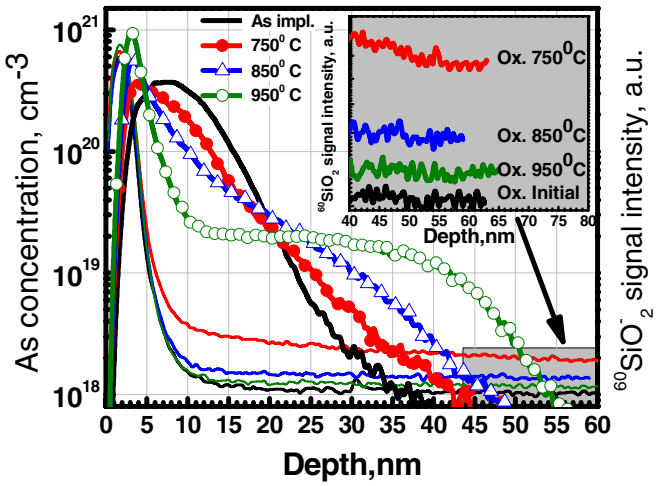

Figure 1. SIMS depth profiles of As and $^{60}SiO_2$ distributions at various annealing temperatures. Inset shows changes in the oxygen concentration at the tail of As depth profile.

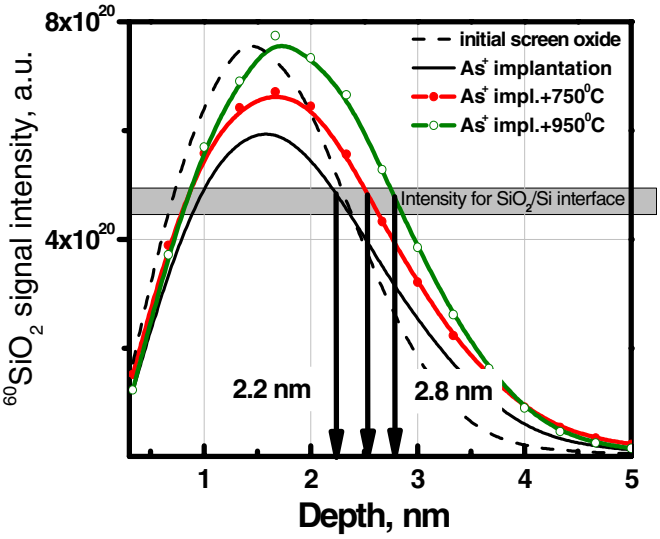

Figure 2. ToF-SIMS depth profile of $^{60}SiO_2$ signal at the SiO_2/Si interface before and after annealing at various temperatures (5 min).

limit for the used SIMS measurements regime amounts to about 4 × 10^{18} cm^{-3} as determined by SIMS investigations of Si reference samples implanted with different doses of oxygen ions. Figure 1 shows an increase in SiO_2 signal by a factor of 2 to 2.5 after anneals at 750 °C compared to the initial value. Therefore, one may estimate that the concentration of oxygen after annealing in the ADR increases up to 1 × 10^{19} cm^{-3}.

Figure 2 shows the $^{60}SiO_2$ signal depth profiles near the SiO_2/Si interface before and after implantation and thermal treatments. It is seen that As implantation leads to decrease in the oxygen concentration within the screen silicon oxide and to some increase of the oxygen concentration in the Si subsurface layer. This effect is related with removal of the oxygen atoms by sputtering at the oxide-vacuum interface and recoil implantation of oxygen atoms from the screen oxide into the underlying silicon substrate [12].

Annealing of the As-implanted samples leads to the increase of the screen silicon oxide thickness and to a recovery of the surface film to the SiO_2 composition. Estimation of the

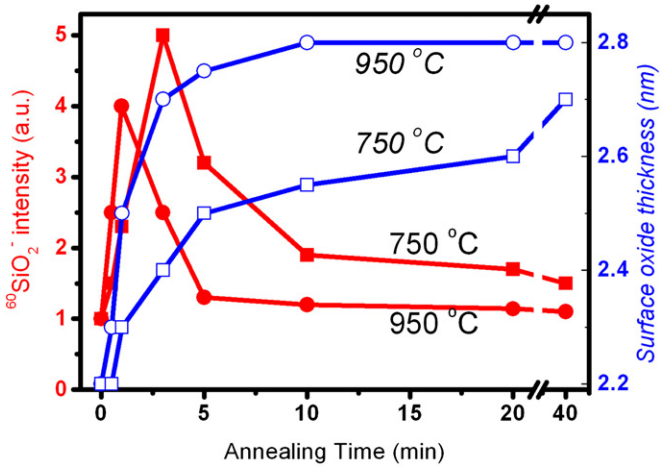

Figure 3. Time dependence of the relative oxygen concentration (filled symbols) in the ADR, and the thickness of surface oxide (open symbols) after annealing.

oxide thickness at the 0.707 level from the maximum of the initial oxygen depth profile shows that the increase of annealing temperature leads to an increase in the screen silicon oxide thickness from 2.2 up to 2.8 nm. This effect is most probably due to additional oxygen supplied from some external source. The origin of this source (annealing atmosphere or Si bulk) is not clear. Part of this redistribution of oxygen can be associated with oxygen gettering to the As implanted region from the bulk of Si wafer. Figure 3 shows time dependences of the $^{60}SiO_2$ intensity in the ADR and the silicon oxide thickness after annealing at 750 and 950 °C. It is seen that the maxima of oxygen concentration in the ADR are reached after 1 and 3 min annealing at 950 and 750 °C, correspondingly. For longer annealing times, the oxygen concentration decreases in the ADR. This oxygen concentration decrease is accompanied by an increase of the surface oxide thickness.

One can see from figure 3 that oxygen accumulation (gettering) processes in the ADR happens during the initial stage of annealing. After that, the process of the surface oxide film growth due to absorption of oxygen from the ADR begins. Just for these time intervals the processes of implanted As redistribution and activation [2, 3] take place suggesting that both the oxygen and As redistribution are correlated. To clarify this correlation, one can compare the time dependence of As and oxygen redistribution during the annealing processes more in detail. As depth profiles determined by SIMS before and after annealing at 750 °C and 950 °C for different times are shown in figure 4.

At T = 750 °C, a significant As redistribution toward the surface occurs only after 5 min annealing, and As accumulation at the SiO_2–Si interface only for anneals longer than 20 min. At T = 950 °C, a substantial As accumulation at the interface begins already after 0.5 min annealing. Comparing figure 4 with figure 3 clearly shows that the time dependences of As interface segregation and of screen oxide thickness growth are strongly correlated.

The observed growth of the oxide thickness requires about 10^{15} cm^{-2} oxygen atoms. Assuming that all this oxygen comes from the substrate, it has to be gettered from a layer thickness of about 12 μm from the surface assuming a concentration of oxygen in the bulk of 10^{18} cm^{-3}. Taking into account that the gettering time of oxygen from such depth amounts to about 5 min at 950 °C, the oxygen diffusivity is estimated to be about 1×10^{-10} cm^2 s^{-1}. This is about an order of magnitude larger than the typical value close to 7×10^{-12} cm^2 s^{-1} [17]. We suppose that it may partly be related with the tensile mechanical stresses related to the very large concentration of As substitutional atoms in the near surface layer and partly to diffusion of OV pairs toward the surface.

Figure 5 shows the normalized $I(q)$ intensities of XDS curves for As-implanted samples before and after annealing at the temperatures 750 to 950 °C for 5 min (*a*) and after annealing at the temperature 750 °C for various times (*b*).

The **q** vector components in the diffraction plane are related with the experimental conditions by the following expression:

$$(\mathbf{q}_z, \mathbf{q}_x) = (\eta \cos \vartheta_B (2\Delta\alpha - \Delta\eta) \sin \vartheta_B)/\lambda, \qquad (1)$$

where λ is the x-ray wavelength, η and $\Delta\alpha$ are angle deviations of the analyzer and monochromator, correspondingly, ϑ_B is the Bragg angle; *Z*-axis is directed normally to the surface, and *X*-axis is parallel to the sample surface; these angles are disposed within the diffraction plane [18].

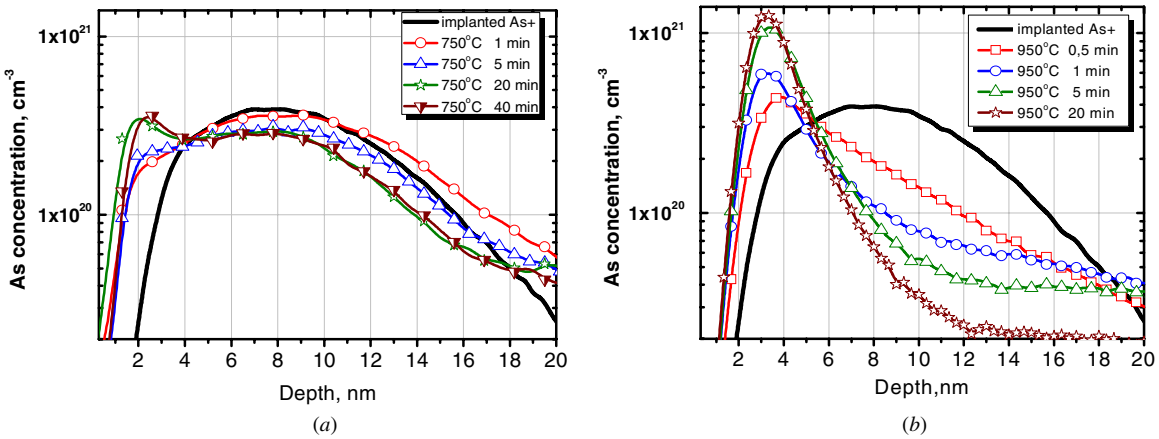

Figure 4. SIMS As depth profiles before and after annealing at 750 (*a*) and 950 °C (*b*).

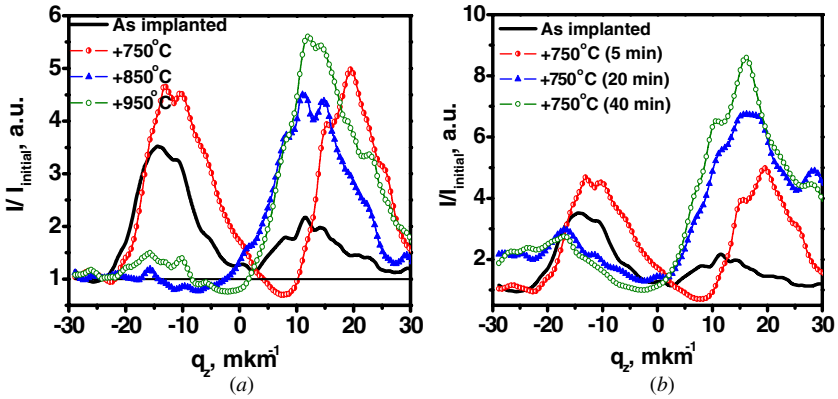

Figure 5. XDS curves for As-implanted samples before and after annealing at the temperatures of 750–950 °C for 5 min (*a*) and after annealing at the temperature of 750 °C for various times (*b*).

The method for determination of the defect concentration consists in finding the Huang and thermo-diffuse scattering ratio with account of the influence of the scattering layer thickness, structure amplitude, spatial angle of scattering, and Debye–Waller factor. So, such important parameters as the micro-defect symmetry, dimension, and concentration may be directly determined from experimental data according to diffuse scattering observed in the investigated sample.

The shapes of curves indicate that all the samples have the defects both of vacancy ($q_z < 0$), and interstitial ($q_z > 0$) types, where q_z is the reciprocal lattice vector. The concentration of both types of defects increases after annealing at 750 °C. After annealing at the temperature 950 °C, the vacancy defects almost disappear, but the concentration of interstitial defects increases.

The XDS curves also indicate the existence of high mechanical stresses in the As implantation region [19]. The components of vector **q** are related to angular deviation of exact Bragg's angle $\Delta\vartheta = \vartheta - \vartheta_B$ with ϑ_B being the Bragg angle. $\Delta\vec{q} \propto \Delta\vartheta \cdot \cos\vartheta/\lambda$ with λ being the x-ray wavelength. The relative change of lattice parameter is $\Delta a/a = -ctg\vartheta \cdot \Delta\vartheta$. In crystal, ion implantation forms both the tensile ($\Delta a/a = 7.7 \times 10^{-4}$) and compressive ($\Delta a/a = -5.64 \times 10^{-4}$) strain regions where a is the Si lattice parameter. Annealing leads to strain redistribution. It can be seen that the size of the tensile strain region is enlarged (figure 5(*a*)) with a slight decrease in the stress after annealing at 750 °C. Simultaneously, the compressive stress is enhanced. The tensile strains disappear after annealing at 850–950 °C. At the same time, the extent of compressive strain region is enlarged with a slight decrease in the stress.

At the beginning of the low-temperature (750 °C) annealing process, reconstruction of implanted region defect structure occurs (figure 5), and concurrently oxygen gettering from the wafer bulk takes place (figure 3). The driving factors for oxygen gettering in the ADR are the tensile mechanical stress gradient in the near-surface region with maximum As concentration.

For anneals longer than 20 min, only a fraction of As atoms are located in substitutional lattice sites, while the rest of the As atoms are accumulated at the SiO_2–Si interface (figure 4(*a*)). The tensile mechanical stress value in the ADR decreases (figure 5(*b*)), and the gettered oxygen flow from the bulk diminishes. The accumulated oxygen atoms in the ADR are pushed to the SiO_2/Si interface (figure 3). The growing surface of SiO_2 layer generates silicon interstitials and also a reorganization of the end of range intersititials into larger defects takes place. These processes lead to an increasing intensity for the positive q_z values in the XRD spectra (figure 5(*b*)).

For annealing at 950 °C, all these processes occur so quickly that separation of them (like in the case of annealing at 750 °C) is impossible. Even after half-minute annealing, one can see all three processes: As segregation (figure 4(*b*)), accumulation of oxygen in the ADR, and an increase of the SiO_2 thickness (figure 3). The reason for this is that after 5 min of annealing at 950 °C the processes of oxygen accumulation and growth of the SiO_2 surface layer are almost completed, and only As diffusion takes place during further anneal.

In our experiments all the anneals were carried out in a high-purity nitrogen ambient, and oxygen supply to the SiO_2/Si interface from the ambient is therefore unlikely. According to SRIM [20] calculations the oxygen recoil generated from the screen silicon oxide during As implantation also does not lead to an appreciable growth of the oxygen concentration within the ADR. So, one can assume that the bulk of the silicon wafer is the main source of oxygen to explain the observed oxide layer growth. In this case, the shallow-implanted As acts as a getter layer for the oxygen in the bulk of the wafer. To confirm this idea, an ^{18}O marker layer was introduced at a depth of 0.3 μm from the sample surface. This buried layer can act as an oxygen source during the anneals. It is necessary to use ^{18}O isotope to be able to separate the implanted oxygen from the background ^{16}O oxygen already present in the wafer.

Figure 6 shows SIMS depth profiles of the implanted ^{18}O atoms before and after annealing at the temperature 950 °C for 5 min in the As-implanted silicon. The projected range of oxygen was close to 300 nm. It is seen that the implanted ^{18}O is strongly redistributed toward the As-implanted surface and incorporates into surface screen oxide layer. It should be noted that the gettering of oxygen on the surface does not occur in the case of only $^{18}O^+$ implantation (figure 6, squares) without prior As implantation.

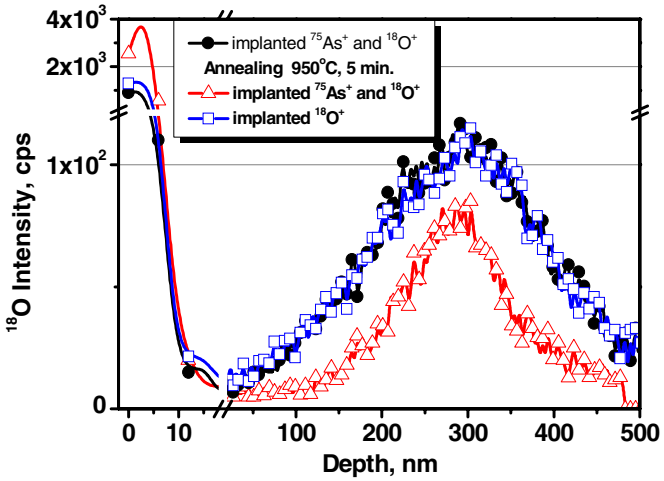

Figure 6. SIMS ^{18}O depth profiles for samples: implanted by $^{75}As^+$ and $^{18}O^+$ without annealing (•); implanted by $^{18}O^+$ (□) and implanted by $^{75}As^+$ and $^{18}O^+$ (△) with subsequent annealing at 950 °C, 5 min.

Discussion

Implanted impurity redistribution occurs toward the screen oxide–Si interface. Therefore, the dopant redistribution processes in this region are examined more in detail. The SIMS depth profiles of $^{60}SiO_2$, ^{18}O and $^{103}AsSi$ signals of the ion distributions are shown in figure 7 for the samples, implanted with As only (*a*) and (*b*) and additionally implanted with ^{18}O isotope (*c*) and (*d*), before and after annealing at 950 °C. One can see that additional implantation of the ^{18}O isotope does not produce noticeable changes in the component distribution over the subsurface area (thickness of ∼12 nm). After annealing of the samples implanted only by As, it is observed that As accumulates at the Si–SiO_2 interface, and that also some (∼0.5 nm) broadening of the ^{18}O and $^{60}SiO_2$ distribution profiles occurs. In the samples with additional implantation of ^{18}O (figure 6), one can observe a considerable (>1 nm) broadening of the ^{18}O distribution profiles and an increase of the integral ^{18}O ion yield by a factor of 4. This is related with the gettering of ^{18}O to the surface screen oxide layer from the bulk of the wafer, whereby the concentration of the implanted ^{18}O decreases by more than a factor of 2 (figure 6). Comparison of the $^{60}SiO_2$ signal depth profiles for the annealed samples (figures 7(*b*) and (*d*)) reveals a significant broadening of the $^{28}Si^{16}O_2$ oxide thickness for the ^{18}O implanted sample. So, the increase of surface oxide thickness occurs not only due to the gettering of ^{18}O but also due to additional ^{16}O atoms outdiffusing from the bulk of the wafer. It may be caused by the following two reasons: enhancement of the gettering of the background oxygen as a result of just ^{18}O implantation or as a result of co-implantation of $^{18}(H_2{}^{16}O)^+$ ions. Co-implantation of monatomic and polyatomic ions can occur due to the low mass resolution of the implanter device.

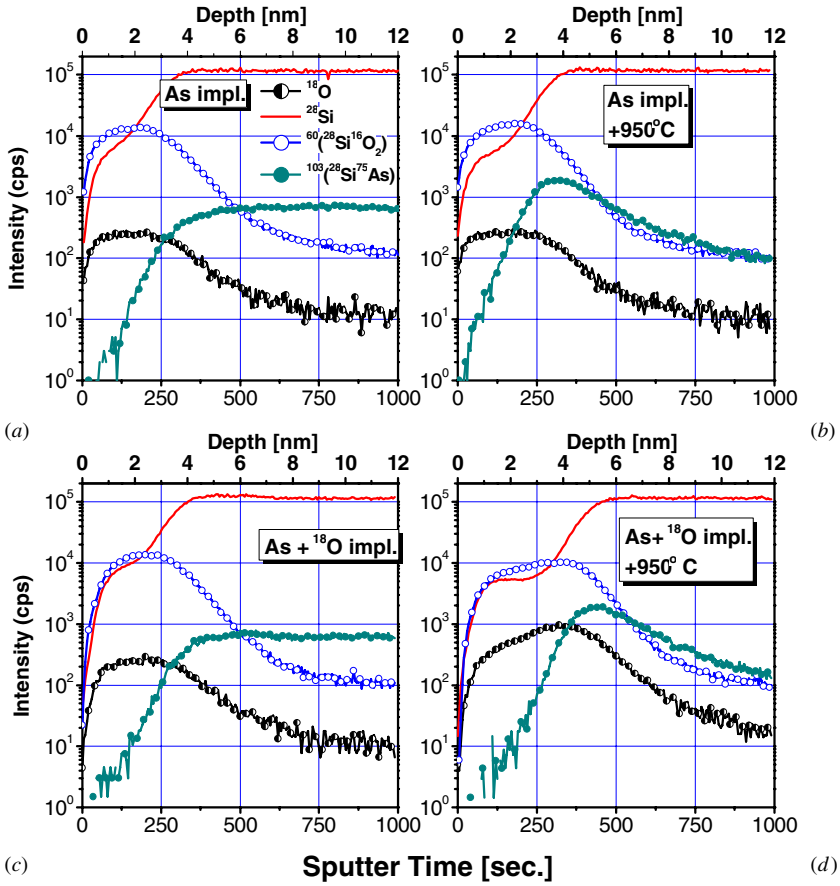

Figure 7. ToF-SIMS depth profiles of $^{60}SiO_2$, ^{18}O and $^{103}AsSi$ signals for the samples implanted by As^+ (*a*) and (*b*) and by As^+ and $^{18}O^+$ (*c*) and (*d*), before (*a*) and (*c*) and after (*b*) and (*d*) annealing at 950 °C, 5 min.

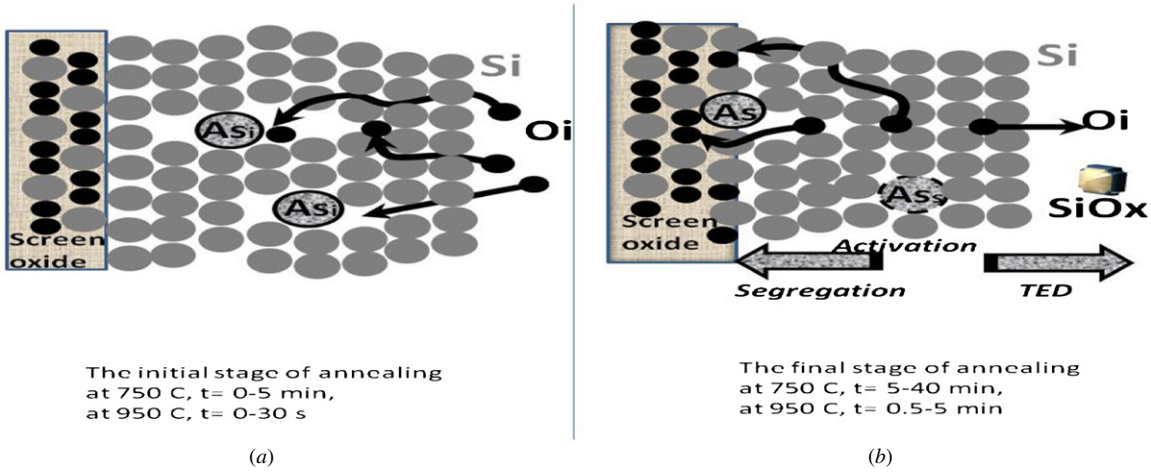

Figure 8. Model of the processes in the As-implanted surface layer during the early (*a*) and final (*b*) stages of annealing.

Thus, the USJ formation after low-energy ion implantation is followed by an increase of the oxygen concentration in the As distribution region. With the increase of the annealing temperature from 750 up to 950 °C, the accumulated oxygen concentration in the As distribution region decreases. However, an increase of the oxide thickness with the annealing temperature is observed. Increasing the annealing time also increases the thickness of the surface oxide. Our model experiments clearly show that during thermal annealing, implanted ^{18}O diffuses from the depth of ~300 nm toward the surface and accumulates at the Si–SiO_2 interface region, indicating the gettering effect.

If one considers the appearance of the peaks in $^{60}SiO_2^-$ signal (figure 3) as a result of the formation of SiO_2 precipitates in the As-rich region the intensities of these peaks as functions of temperature can be explained as follows. It is well-known that the critical radius of the formation of SiO_2 precipitate depends not only on the supersaturation of interstitial oxygen but also on the supersaturation of the intrinsic point defects, both vacancies and Si self-interstitials [9]:

$$R_{\mathrm{cr}} = \frac{2\sigma\Omega}{kT \ln \frac{C}{C_{\mathrm{eq}}} \left(\frac{V}{V_{\mathrm{eq}}}\right)^{\beta} \left(\frac{I}{I_{\mathrm{eq}}}\right)^{-\gamma}} \qquad (2)$$

where σ (= 0.43 J m^{-2} for SiO_2) is the specific energy of the interface of the SiO_x precipitate with the Si matrix [21], Ω (= 2.25 × 10^{-29} m^3 for SiO_2) is the volume per oxygen atom in the silicon oxide phase [22], k is the Boltzmann constant, T is the temperature, C, V, and I are the concentrations of interstitial oxygen, vacancies, and Si self-interstitials, respectively, and C_{eq}, V_{eq}, and I_{eq} are their equilibrium concentrations, respectively [9, 23]. β and γ are the number of vacancies and interstitials, respectively, absorbed in the precipitate per precipitated oxygen atom. Here one should take into account that the formation energies of the intrinsic point defects also depend strongly on the Fermi level position and to some extent also on the stress introduced by the large concentration of substitutional dopant atoms [24, 25].

As follows from equation (2), a supersaturation with vacancies leads to enhanced precipitation due to the decrease of the critical radius R_{cr}. The higher vacancy supersaturation at 750 °C due to the lower vacancy solubility V_{eq} combined with the higher supersaturation of oxygen, probably explains the higher intensity of $^{60}SiO_2^-$ signal peak comparing to that at 950 °C. Another reason may be higher rate of activation of implanted As at 950 °C leading to the decrease of vacancy concentration and, hence, a decrease of the vacancy supersaturation. In addition, the oxygen concentration driven into the region of As evolution is higher at 750 °C which, together with smaller oxygen solubility, realizes higher oxygen supersaturation and additional decrease of the critical radius for SiO_x precipitation.

In the considered view a decrease in the intensity of $^{60}SiO_2^-$ signal at longer annealing times may be attributed to the dissolution of SiO_x precipitates due to energetically more favorable oxidation of a surface SiO_2 layer as well as due to the possible increase of the concentration of Si self-interstitials produced by such oxidation, which leads to the increase of the critical radius for precipitation (see equation (2)). A tentative model for the kinetic processes occurring in the As-implanted surface layer at the early stage of annealing is shown in figure 8(*a*). At the initial stage of annealing after rapid recombination of part of the implantation induced intrinsic point defects, As is in the metastable interstitial position, creating a tensile stress of the surface layer, which contributes to oxygen gettering from the wafer bulk to the heavily As doped near-surface layer during the anneal. At 750 °C, this process goes on for about 3 to 6 min. Longer annealing (figure 1(*b*)) leads to activation of part of the As atoms (= they are now substitutional), while the other part is accumulated at the SiO_2–Si interface after rapid diffusion of interstitial As atoms. The tensile stresses decrease (figure 5), the enhanced oxygen flow from the bulk is terminated, and oxygen diffuses gradually from ADR to the Si–SiO_2 interface, increasing the thickness of the surface oxide. At higher annealing temperatures (950 °C), these processes of restructuring of the surface layer and oxygen gettering from the wafer bulk occur over a much shorter time period (<1 min.).

The growth of the thickness of the oxide surface layer occurs due to absorption of gettered oxygen for a time from

1 to 5 min. Further annealing at 950 °C leads to a change in the As distribution profile partly due to interaction of point defects. Oxygen atoms do not participate in these processes.

Conclusions

Point defect stimulated gettering of oxygen during thermal activation of implanted As in silicon has been observed. The dependence of As and oxygen depth profiles on thermal anneal temperature and duration have been investigated. An increase of the surface oxide thickness during annealing was observed and was explained by oxygen gettering from the Si wafer bulk toward the USJ region. This effect was confirmed by a model experiment with additional implantation of $^{18}O^{+}$ ions into Si substrate. It was shown that implanted ^{18}O atoms are strongly redistributed toward the As-implanted surface, and incorporated into the surface screen oxide layer. Oxygen redistribution is related with the tensile mechanical stresses, and vacancy concentration distribution in implanted Si. This surface layer 'purification' from oxygen provides a positive influence on the parameters of nano-devices. The influence of point defects, both vacancies and interstitials, on the process of formation of impurity precipitates during formation of ultrashallow junctions was also considered.

References

[1] ITRS 2012 International Technology Roadmap for Semiconductors www.itrs.net/Links/2012ITRS/2012Chapters/2012Overview.pdf

[2] Kruger D, Rucker H, Heinemann B, Melnik V, Kurps R and Bolze D 2004 Diffusion and segregation of shallow As and Sb junctions in silicon *J. Vac. Sci. Technol.* **22** 455

[3] Rucker H, Heinemann B, Barth R, Bolze D, Melnik V, Kurps R and Kruger D 2003 Formation of shallow source/drain extensions for metal-oxide-semiconductor field-effect-transistors by antimony implantation *Appl. Phys. Lett.* **82** 826

[4] Ural A, Griffin P and Plummer J 1999 Fractional contributions of microscopic diffusion mechanisms for common dopants and self-diffusion in silicon *J. Appl. Phys.* **85** 6440

[5] Solmi S, Ferri M, Bersani M, Giubertoni D and Soncini V 2003 Transient enhanced diffusion of arsenic in silicon *J. Appl. Phys.* **94** 4950

[6] Shibahara K, Furumoto H, Egusa K, Koh M and Yokohama S 1998 Dopant loss origins of low energy implanted arsenic and antimony for ultra shallow junction formation *Mater. Res. Soc. Symp. Proc.* **532** 23

[7] Shirai H, Yamaguchi A and Shimura F 1996 Effect of back-surface polycrystalline silicon layer on oxygen precipitation in Czochralski silicon wafers *Appl. Phys. Lett.* **54** 1748

[8] Falster R, Fisher G R and Ferrero G 1991 Gettering thresholds for transition metals by oxygen-related defects in silicon *Appl. Phys. Lett.* **59** 809

[9] Vanhellemont J and Claeys C 1987 A theoretical study of the critical radius of precipitates and its application to silicon oxide in silicon *J. Appl. Phys.* **62** 3960

[10] Magee T J, Leung C, Kawayoshi H, Palkuti L J, Furman B K, Evans C A, Christel L A, Gibbons J F and Day D S 1981 Recoil oxygen implants and thermal redistribution of oxygen in through-oxide arsenic-implanted Si *Appl. Phys. Lett.* **39** 564

[11] Zhao Y, Li D, Ma X and Yang D 2004 The effect of the ramping rate on oxygen precipitation and the denuded zone in heavily doped Czochralski silicon *J. Phys.: Condens. Matter* **16** 1539

[12] Baumvol I J R, Stedile F C, Rigo S, Ganem J J and Trimaille I 1994 The effects of ion implantation through very thin silicon oxide films *Braz. J. Phys.* **24** 529

[13] Hirao T, Fuse G, Inoue K, Takanayagi S, Yaegashi Y and Ichikawa S 1979 The effects of the recoil-implanted oxygen in Si on the electrical activation of As after through-oxide implantation *J. Appl. Phys.* **50** 5251

[14] Kögler R, Wieser E, Albrecht J and Knothe P 1989 Investigation of As—O clustering in Si *Phys. Status Solidi* a **113** 321

[15] Lu G-H, Wang Q and Liu F 2008 The role of vacancy on trapping interstitial O in heavily As-doped Si *Appl. Phys. Lett.* **92** 211906

[16] Molodkin V B, Olikhovskii S I, Len E G, Kislovskii E N, Kladko V P, Reshetnyk O V, Vladimirova T P and Sheludchenko B V 2009 Sensitivity of triple-crystal X-ray diffractometers to microdefects in silicon *Phys. Status Solidi* a **206** 1761

[17] Newman R C 2000 Oxygen diffusion and precipitation in Czochralski silicon *J. Phys.: Condens. Matter* **12** R335

[18] Kladko V P, Datsenko L I, Bak-Misiuk J, Olikhovskii S I, Machulin V F, Prokopenko I V, Molodkin V B and Maksimenko Z V 2001 Calculation of two-dimensional maps of diffuse scattering by a real crystal with microdefects and comparison of results obtained from three-crystal diffractometry *J. Phys. D: Appl. Phys* **34** A87

[19] Gudymenko O I, Kladko V P, Melnik V P, Olikh Ya M, Popov V G, Romanyuk B M, Slobodian M V and Kogutyuk P P 2008 Peculiarities of the defect formation in the near-surface layers of Si single crystals under acoustostimulated implantation of ions of boron and arsenic *Ukr. J. Phys.* **53** 140

[20] Ziegler J F 2004 SRIM-2003 *Nucl. Instrum. Methods* B **219–220** 1027

[21] Borghesi A, Pivac B, Sassella A and Stella A 1995 Oxygen precipitation in silicon *J. Appl. Phys.* **77** 4169

[22] Litovchenko V G, Lisovskyy I P, Kladko V P, Zlobin S O, Muravs'ka M V, Efremov A A and Slobodyan M V 2007 Influence of defects on the structure of oxygen precipitates in silicon crystals *Ukr. J. Phys.* **52** 958

[23] Sarikov A, Litovchenko V, Lisovskyy I, Voitovich M, Zlobin S, Kladko V, Slobodyan N, Machulin V and Claeys C 2011 Mechanisms of oxygen precipitation in Cz-Si wafers subjected to rapid thermal anneals *J. Electrochem. Soc.* **158** H772

[24] Vanhellemont J, Kamiyama E and Sueoka K 2013 Silicon single crystal growth from a melt: on the impact of dopants on the v/G criterion *ECS J. Solid State Sci. Technol.* **2** 166

[25] Sueoka K, Kamiyama E and Vanhellemont J 2013 Density functional theory study on the impact of heavy doping on Si intrinsic point defect properties and implications for single crystal growth from a melt *J. Appl. Phys.* **114** 153510